PAPER

Facile preparation of boron phosphide particles with high purity and high structural stability

Materials Research Express

PAPER

Facile preparation of boron phosphide particles with high purity and high structural stability

RECEIVED
10 September 2019

REVISED
17 November 2019

ACCEPTED FOR PUBLICATION
2 December 2019

PUBLISHED
19 February 2020

Menglei Feng[1], **Jinbo Zhang**[2,3], **Hongpeng Zhou**[1], **Pengfei Jiang**[1], **Dingke Zhang**[4], **Lin Wang**[2] and **Shijian Chen**[1,5]

[1] School of Physics, Chongqing University, 401331, People's Republic of China
[2] Center for High Pressure Science and Technology Advanced Research, Shanghai, 201203, People's Republic of China
[3] College of Physical Science and Technology, Yangzhou University, Yangzhou, 225002, People's Republic of China
[4] College of Physics and Electronic Engineering, Chongqing Normal University, Chongqing, 401331, People's Republic of China
[5] Author to whom any correspondence should be addressed.

E-mail: wanglin@hpstar.ac.cn **and** sjchen@cqu.edu.cn

Keywords: boron phosphide, high pressure, XRD, Raman

Supplementary material for this article is available online

Abstract

In this work, microsized cubic BP particles was produced by vacuum-sealed solid state reaction. X-ray diffraction Rietveld refinement and x-ray photoelectron spectroscopy results indicate the prepared BP particles are highly crystalline and high purity. *In-situ* x-ray diffraction and Raman measurements under high pressure show the cubic BP particles possess high structural stability up to 36.0 GPa with high reversible structure recovering ability. Meanwhile, a high bulk modulus of 205(2) GPa and pressure derivative B_0' of 3.8(1) are obtained from *in situ* x-ray diffraction measurements. Grüneisen parameters of 1.01 and 1.17, and the pressure coefficient $d\omega/dp = 4.07$ and 4.57 cm^{-1}/GPa for LO and TO mode, respectively, are also deduced from Raman measurements under various high pressure.

1. Introduction

Boron monophosphide (BP), an III–V compound with zinc-blende structure, consists of two earth-abundant light elements of boron (B) and phosphorus (P). The electronic charge distribution is nearly symmetrical between the cation and the anion [1], due to a strong covalent bonding between B and P atoms and very low iconicity of III-V compounds ($f_i = 0.006$) [2]. BP material was prepared by P Popper and T A Ingles via reaction of boron and red phosphorus at 1957 [3]. Nowadays, BP material has been widely studied and used in many fields and harsh environments due to its distinct physical and chemical properties like high melting point of 3000 °C, high hardness of 4700 kg mm^{-2}, high mobility of 120 $cm^2s^{-1}V^{-1}$and high thermal stability [4, 5]. In addition, BP possesses considerable chemical stability and is almost resistant to any acid and alkali solution except melt-out NaOH [6]. The unique electronic properties of BP also make it great potential in thermal neutron counter and neutron detector [7]. BP has an indirect gap of 2.0 eV with the valence band maximum (Γ) and conduction band minimum (X) locating at different symmetry points of Brillouin zone, which is suitable for visible light active photocatalyst for hydrogen evolution [8]. In recent studies, BP nanowires were fabricated to make homostructural optoelectronic devices [9] and single crystal BP for high thermal conductivity application [10, 11]. Furthermore, due to the small hole effective mass and high hole mobility, BP material was proposed to be potential as an non-oxide p-type transparent conducting material [12]. Density functional theory (DFT) also predicted that monolayer hexagonal BP can be a potential anode material for alkali metal-based batteries [13] as well as tuning different electronic properties by doping [14, 15].

As far as we know, BP had been synthesized with many traditional methods by far. The most commonly used way was chemical vapor deposition [16–18], in which B_2H_6 (1% in hydrogen) and PH_3 (5% in hydrogen) were reacted in a high temperature condition. BP powders were also prepared from mixed boron and zinc phosphide in quartz tube at elevated temperature [8, 19]. Single crystal BP was prepared by direct reaction of elemental

boron and phosphorus with the use of Sn or Ni as catalyst [10, 20]. Recently, mechanochemical methods for the synthesis of fine boron phosphide powders with the nominal purity higher than 97% was reported [21]. However, all these mentioned methods have disadvantages, such as use of toxic reagents, low yield and poor purity of BP products.

In the meantime, the study of materials on the pressure-induced structure phase stability is of very importance in interdisciplinary areas, such as physics [22], chemistry [23], and biology [24], etc. The crystal structure changes of the material can be affected by high pressure, such as the reduced interatomic distance and even the occurrence of structure phase transition up to certain pressure. However, there is seldom work on the structure phase stability and physical properties of cubic BP under high pressure. In this regard, it is very meaning for studying the dynamic process of pressure-induced crystal structure phase stability of BP particles.

In this work, we propose a simple and low-cost way to synthesize BP material with high purity and high yield. Solid-phase reaction without using any cocatalysts not only produced BP particles with high purity, but also ensured high yield. Meanwhile, we also have studied the crystal structure phase stability of the prepared BP particles under high pressure by *in situ* x-ray diffraction and Raman spectroscopy, which showed that the BP structure was stable up to 36.0 GPa hydrostatic pressure (which is the highest pressure that can be obtained in our set-up) with high reversible recovered ability and showed no structure phase transitions. Meanwhile, through the least-squares fitting and numerical calculation results, the bulk modulus $B_0 = 205(2)$ GPa and its pressure derivative $B_0' = 3.8(1)$ at zero pressure, and the Grüneisen parameter γ_{LO} and γ_{TO} are 1.01 and 1.17 with the pressure coefficient $d\omega/dp = 4.07$ and 4.57 cm^{-1}/GPa, respectively.

2. Experimental section

2.1. Synthesis of BP powder

The boron (Aladdin CAS: 7440-42-8) and red phosphorus (Alfa Aesar CAS: 7723-14-0) with the mole rate of 1:1 were adequately mixed and carefully grounded in the agate mortar for about 10–15 min, and the mixed powders were immediately sealed in a quartz tube under 3.0×10^{-4} Pa. The sealed quartz tube was placed into the muffle reaction furnace and heated up to 1100 °C at the heating rate of 5 °C/min, and kept at 1100 °C for 12 h, then naturally cooled down to room temperature. The as-synthesized powders were treated with concentrated HNO_3 for 0.5 h at a 70 °C bath temperature for removing the incompletely reacted B and red P, then the solution was centrifuged and washed thoroughly with deionized water for several times. And diluted NaOH solution was used to remove white H_3BO_3, then the BP powders were annealed under Ar atmosphere at 500 °C for 3 h to sublime phosphorus impurity. Eventually, high-purity BP powders were successfully synthesized and the total yield of BP sample can be up to 90%–95%. Compared with the traditional methods, the developed method can synthesize high purity and highly crystalline BP particles with high yield so that it is great potential for large-scale application in practical use.

2.2. Characterization

The crystal structure analysis of the BP powder was performed using an X'Pert PRO diffractometer (PANalytical) operated with a Cu $K\alpha_1$ x-ray source ($\lambda = 1.5406$ Å) at an accelerating voltage of 40 KV and an applied current of 40 mA. The microscopic morphologies and structures of the BP sample was analyzed by scanning electron microscope (SEM) and transmission electron microscope (TEM, FEITenaiTM F30). The phase purity and elemental valence states of the powders were measured by x-ray photoelectron spectroscopy (XPS, Kratos AXIS UltraDLD) with Al $K\alpha$ radiation as the excitation source and the energy calibrations were referenced C1s peak at 284.8 eV. The optical absorption spectrum in the 300–800 nm range was measured by UV-visible spectrophotometer (Shimadzu UV3600). High-pressure synchrotron x-ray diffraction experiments were carried out at the Shanghai Synchrotron Radiation Facility (SSRF, BL15U1 beamline), China. The energy of high-energy x-ray source was 20 KeV ($\lambda = 0.6199$ Å). The symmetric diamond-anvil cell (DAC) was used to generate high pressure, and the prepared BP powder was stuck on the needle tip and set in the sample chamber of 130 μm diameter and compressed between 300 μm diameter culet DAC. Silicon oil was used as pressure-transmitting medium, T301 standard steel sheet with thickness of 250 μm was used as gasket, and pressure determination was achieved by the hydrostatic ruby scale. The two-dimensional XRD images were collected with a charge-couple device (CCD MAR 165) detector, the 2D ring-type images were integrated using Dioptas software. High pressure Raman spectrum was conducted on the LabRAM HR Evolution spectrometer (HORIBA Jobin Yvon) with the 532 nm excitation source, and a 2400 G mm^{-1} optical grating was used. In addition, the Gauss*Lorentz function and Pearson function were used to fit the peak profiles of XRD and Raman spectrum, respectively.

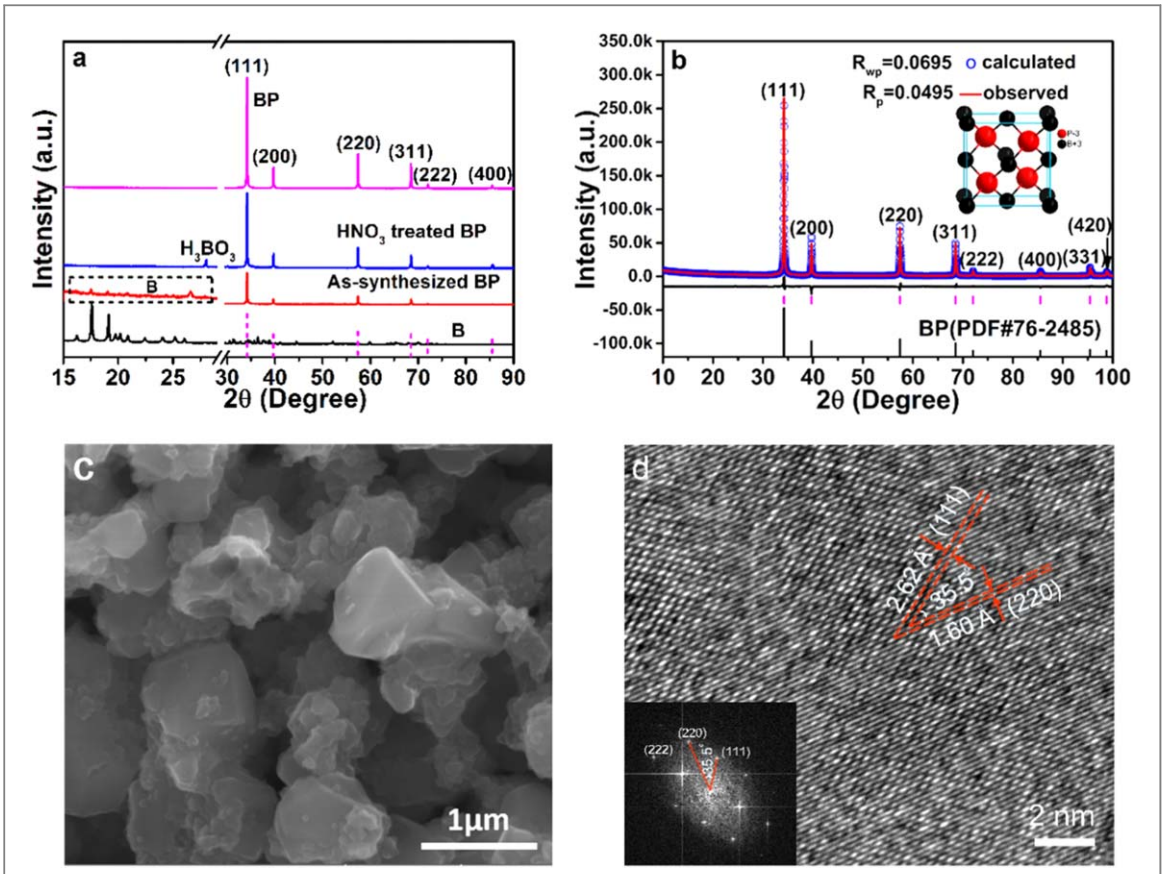

Figure 1. (a) The XRD patterns of BP sample at different preparation stages. (b) Rietveld refinement plot of final product BP with the unit cell (inset). (c) SEM image and (d) HRTEM image of BP particle with the corresponding Fast-Fourier transform (FFT) pattern in the inset.

3. Results and discussion

3.1. Structure and morphology analysis

XRD patterns were measured to characterize the structure and phase purity of BP sample at different preparation stage. As shown in figure 1(a), for the as-synthesized BP powder, though BP was the main product in the powder, there was still race of elemental B existed in the sample which contributed to the weak diffraction peaks appearing in the 2θ angle range of $15 \sim 30°$. After the powder was treated with concentrated HNO_3, elemental B was successfully removed, but the reactive product H_3BO_3 was existed in the sample. So the samples were treated with NaOH solution and then annealed under Ar atmosphere to remove H_3BO_3 and extra P, respectively. The final products of high purity BP were obtained. The prepared BP powders possessed four major typical diffraction peaks located at $2\theta = 34.2°, 39.7°, 57.4°$ and $68.5°$ which were assigned to (111), (200), (220) and (311) planes of cubic BP [8, 20]. The very sharp XRD peaks with full-width half-maximum (FWHM) of 0.078° for (111) peak suggested very high crystallinity of our prepared BP. The absence of any impurity peaks such as B and red P in the XRD pattern indicating the high purity of BP. As far as we know, B_6P phase would appear as BP is heated at elevated temperature (about 1100 °C) under reduced pressure due to the loss of phosphorus [25, 26]. However, there was no B_6P impurity phase in the XRD patterns, which suggested that the prepared BP sample presented superior thermal stability. In order to clarify the high crystallinity and phase purity of our prepared BP sample, the high-resolution XRD data for Rietveld refinements were collected with a setting of 200 s 0.0131°, the Rietveld refinements were performed with the software package of TOPAS (figure 1(b)). The refinement results indicated all the diffraction peaks in the experimental data were fitted well by the Rietveld theoretical model, and the differences between experimental and theoretical data were very small. The small agreement factors (Rwp, Rp) also indicated the high crystallinity of the prepared BP. BP has the zinc-blende structure with the space group F-43m, and lattice parameters of BP are 4.55 Å [3]. The calculated lattice parameters $a = b = c = 4.53781(8)$ Å from observed diffraction peaks were very close to the reported values [3] and the prepared BP is of single cubic phase. Figure 1(c) showed the obtained BP presented polyhedral particles with a size of about 1 micrometer. HRTEM image (figure 1(d)) showed two obvious plane spacing of 0.262 nm and 0.160 nm, corresponding to (111) and (220) plane of cubic BP, respectively [9, 27]. The well

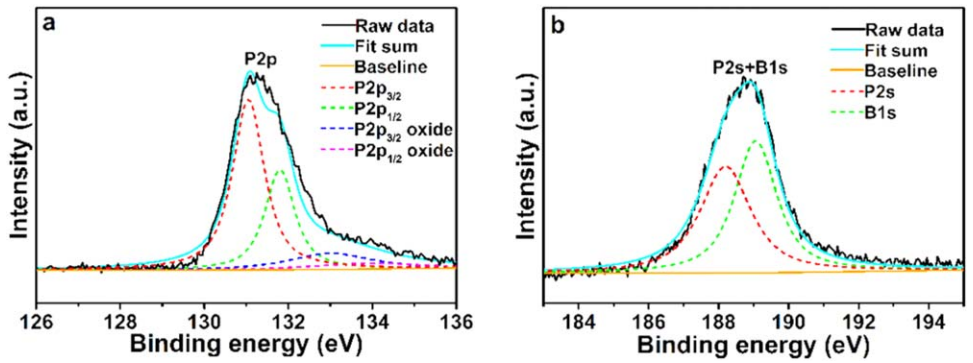

Figure 2. High-resolution spectra of XPS signals: (a) P 2p and (b) P 2 s + B 1 s signals of the prepared BP sample.

resolved lattice fringes and clear FFT pattern taken from HRTEM further confirmed the high crystallinity of the prepared BP. Meanwhile, the absorption spectrum of the prepared BP powder showed the light absorption edge was approximately 620 nm with the indirect gap of 2.0 eV (figure S1 in supplementary information is available online at stacks.iop.org/MRX/6/125922/mmedia).

3.2. Element analysis

In order to study phase purity of the prepared BP samples, XPS high-resolution spectra of B 1 s and P 2p core level were plotted in figure 2, taking the Tougaard background into consideration. The B 1 s and P 2p peaks were located at binding energies of 189.0 and 131.0 eV, respectively, which were in consistent with the reported value of cubic BP [8, 9, 28]. The P 2p core-level was splitted naturally into two distinct core states P $2p_{3/2}$ and P $2p_{1/2}$ due to the spin-coupling. Meanwhile, the presence of weak P 2p signals of oxidized phosphorus indicated that tiny oxygen were incorporated in the BP sample due to exposure to ambient conditions [27–29]. Since the binding energy of B 1 s is very closed to that of P 2 s, the B 1 s + P 2 s signals (figure 2(b)) consisted of the overlapping distribution of electrons excited from B 1 s and P 2 s core-level [9]. The above XPS results indicated a single phase of cubic BP with high purity.

3.3. High-pressure structure analysis

It is well known that pressure is the most effective way to change the interatomic distances and influence the crystal structure phase stability. The DFT study found that the phase transition of BP from the zinc-blende to rocksalt structure occurred at 142 GPa [30], and the experiment results reported by Arthur L. Ruoff indicated that BP remained stable zinc-blende structure phase up to at least 110 GPa [2]. Figure 3(a) showed that the XRD pattern of the hydrostatic pressure varied from 0.16 to 36.0 GPa and released back to 0.73 GPa, the results indicated the BP cubic structure phase remained stable when the pressure raised up to 36.0 GPa, which was the highest pressure we could reach in our lab. In terms of the Bragg diffraction formula $2d\sin\theta = n\lambda$, the diffraction peak positions were shifted to higher 2θ diffraction angle due to the increased pressure and decreased interatomic distance. In addition, as the pressure increased from 0.15 GPa up to 36.0 GPa, the diffraction peaks gradually became broad, weak but no extra peaks related to other phases were observed, which showed no structural transition under the pressure up to 36.0 GPa. As the pressure was sequentially released from 36.0 back to 22.80, 5.56 and 0.73 GPa, the diffraction peaks were shifted back to lower diffraction angle and became narrower and stronger, which stated the cubic BP structure possessed a high reversible recovering ability. The experimental P-V relation curve was shown in figure 3(b), the third-order Brich-Murnaghan equation of state was used to fit the experimental data by the least-squares fitting [2, 31, 32]:

$$P = 3/2B_0(x^{7/3} - x^{5/3})[1 + 3/4(B_0' - 4)(x^{2/3} - 1)] \quad (1)$$

Where P was the pressure, $x = V_0/V$, the zero-pressure cubic unit cell volume was obtained from the lattice parameter $a = 4.54(3)$ Å and $V_0 = (\sqrt{3} \times 2.62)^3 = 93.45$ Å^3, B_0 is the bulk modulus at zero pressure, and B_0' is the pressure derivative of the bulk modulus evaluated at zero pressure, which give the value of the bulk modulus $B_0 = 205(2)$ GPa with its pressure derivative $B_0' = 3.8(1)$ at zero pressure. The large bulk modulus (205(2) GPa) obtained from our BP particles was greater than the reported values (165, 174, 173 GPa) [2, 32, 33] and less than the value ($B_0 = 267$ GPa) obtained from non-hydrostatic experiment [34]. Bulk modulus, a measure of the hardness of materials, is used to present the resistance to compressibility. The $B_0 = 205(2)$ GPa of the prepared BP was greater than that of other III-phosphide semiconductors, such as AlP, GaP and InP. The large bulk modulus of BP indicated the high hardness and highly incompressible behaviour due to the strong B-P covalent bonding. Meanwhile, the peak position of (111) plane and the lattice constant of BP only shifted by 0.6° and

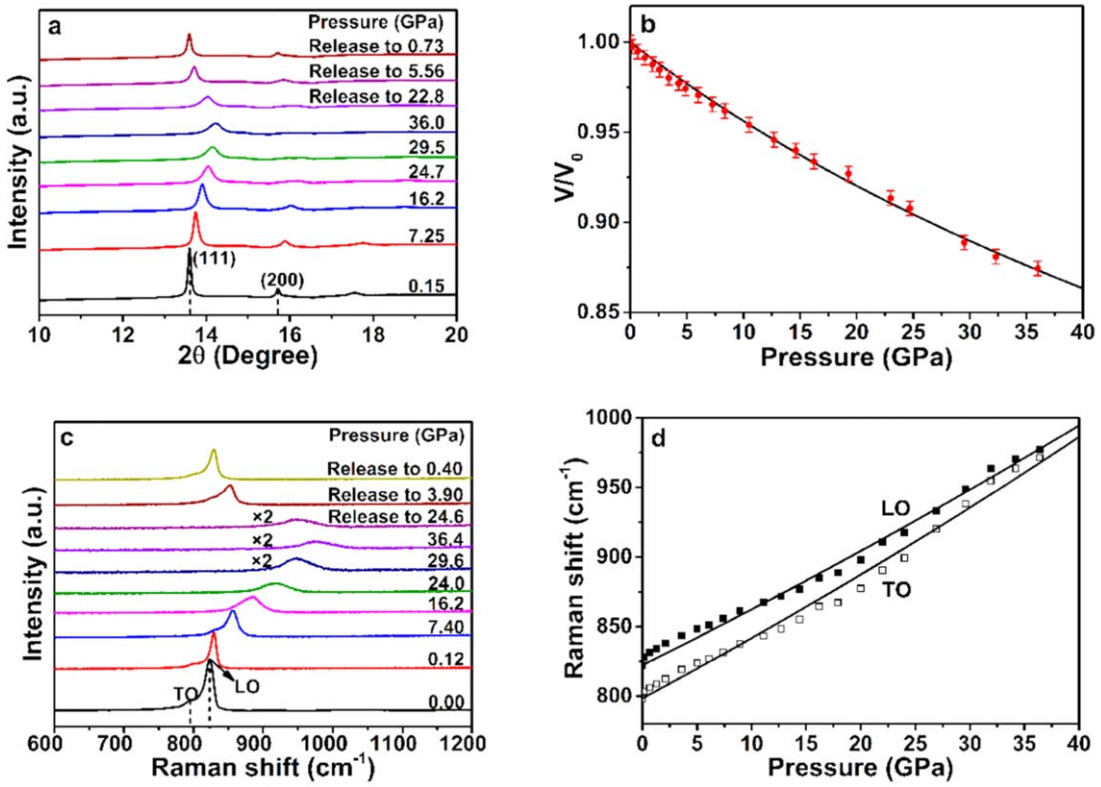

Figure 3. (a) XRD patterns of BP at different hydrostatic pressures. (b) The plot of V/V_0 as a function of pressure. The triangles corresponded to the powder x-ray diffraction data, and the solid line represented a least-squares fitting results using third-order Birch-Murnaghan EOS. (c) Raman spectra of BP under different hydrostatic pressure. (d) The Raman shift of LO and TO virbration mode as a function of pressure, the dependence was fitted by the linear relationship as $\omega(P) = \omega_0 + (d\omega/dp)\,P$.

shrank by 0.113 Å while the pressure varied from 0.15 to 36.0 GPa, further indicating that BP possessed the remarkable mechanical property of high bulk modulus and incompressibility.The unit-cell volume decreased with increasing pressure while the volume diminished by 12% at 36.0 GPa. Furthermore, we found there was no distinct drop of the unit-cell volume observed with the increase of pressure, which indicated the structure phase stability of BP.

To further study the phase stability of the BP crystal structure and vibrational properties of the BP lattice, pressure-dependent Raman spectra was measured (figure 3(c)). The Raman spectrum of BP sample under 0 GPa pressure showed two obvious Raman peaks located at about 798 cm^{-1} and 822 cm^{-1}, corresponding to the transverse optical (TO) and longitudinal optical (LO) mode originated from the vibrations at the highest symmetry point (Γ) in the Brillouin zone [10, 11, 32], which demonstrated the high purity and good crystalline quality of our prepared BP samples. As the pressure increased, the Raman peaks shifted to higher wavenumbers and became broaden and weaken, due to the variation of the interatomic distance [35] and anharmonic interactions affecting phonon lifetime. The atoms move away from their equilibrium atomic positions as the pressure increases, which induces structural deformation and Raman intensity reduction. Analogy to XRD result, we did not observe any additional peaks as the pressure increased up to 36.4 GPa, which indicated no structure phase transition and the structure of BP was stable up to 36.4 GPa (the maximum pressure we can reach). After the highest pressure (36.4 GPa) was gradually released back to 24.6, 3.90 and 0.40 GPa, the Raman spectrum fully recovered to its original frequencies and shapes, which indicated a high reversible recovering ability of the cubic crystal phase of our prepared BP particles. Since these modes correspond to the stretching vibrations of the shorter B-P distances, the observed compressibility changes should reflect the pressure-induced behaviour of the corresponding bond length. We plotted the dependence of the LO and TO frequencies on pressure in figure 3(d) and fitted it with a linear formula [36, 37]:

$$\omega(P) = \omega_0 + (d\omega/dp)P \quad (2)$$

Where ω is the phonon frequency, P is the hydrostatic pressure and $d\omega/dp$ is the pressure coefficient. The relation between phonon frequency and pressure was fitted by the least-squares fits, the equation were

$$\omega_{LO} = 824.8 + 4.07P \quad (3)$$

$$\omega_{TO} = 797.4 + 4.57P \quad (4)$$

The fittted results presented $\omega_0 = 824.8$ and 797.4 cm^{-1} with the postive pressure slope $d\omega/dp = 4.07$ and 4.57 cm^{-1}/GPa for LO and TO mode, respectively. To further obtain the LO and TO mode stiffness, the Grüneisen parameter was calculated by the equation

$$\gamma = -\frac{dln\omega}{dlnV} = \frac{B_0}{\omega_0}\frac{d\omega}{dP} \quad (5)$$

Where γ is Grüneisen parameter, ω_0 is phonon frequency at zero pressure, V is the cell volume, B_0 is the bulk modulus and P is the pressure [36–38]. We obtained the Grüneisen parameter were $\gamma_{LO} = 1.01$ and $\gamma_{TO} = 1.17$, respectively, which were a little less than the reported values [32, 36]. Furthermore, we could conclude that LO-TO splitting reduced with the increasing pressure, which was resulted from the a larger pressure coefficient of TO than that of LO mode.

4. Conclusion

In summary, we have successfully synthesized cubic BP particles with high-purity and high crystallinity by high-temperature vacuum-sealed solid-reaction method and the total yield of BP sample can be up to 90%–95%. The developed method has great potential for large-scale application in practical use due to its low-cost and simple. All the diffraction peaks in the experimental data were fitted well by the Rietveld theoretical model, which indicated the high crystallinity of the prepared cubic BP particles. From the *in situ* high pressure XRD and Raman analysis, we can conclude the BP cubic structure phase is stable up to 36.0 GPa hydrostatic pressure with the reversible structure recovering ability and shows no structure phase transition. The bulk modulus $B_0 = 205(2)$ GPa and $B_0' = 3.8(1)$ with the Grüneisen parameter γ_{LO} =1.01 and $\gamma_{TO} = 1.07$ were fitted by HPXRD and Raman spectras.

Acknowledgments

This work is supported by the National Natural Science Foundation of China (NSFC) (grants 51672031). We thank Mr Xiangnan Gong at Analytical and Testing Centre of Chongqing University for Raman measurement and discussion.

ORCID iDs

Dingke Zhang https://orcid.org/0000-0003-0095-4368
Lin Wang https://orcid.org/0000-0001-8276-7026
Shijian Chen https://orcid.org/0000-0002-9523-6686

References

[1] Leite Alves H W and Kunc K 1992 *J. Phys.: Condens. Matter* **4** 6603
[2] Xia H, Xia Q and Ruoff A L 1993 *J. Appl. Phys.* **74** 1660–2
[3] POPPER P and INGLES T A 1957 *Nature* **179** 1075
[4] Motojima S, Ohtsuka Y, Kawajire S, Takahashi Y and Sugiyama K 1979 *J. Mater. Sci.* **14** 496–8
[5] Stone B and Hill D 1960 *Phys. Rev. Lett.* **4** 282–4
[6] Kumashiro Y 1990 *J. Mater. Res.* **5** 2933–47
[7] Viles T P and Brunett B A 1997 *MRS.* **487** 158–63
[8] Shi L, Li P, Zhou W, Wang T, Chang K, Zhang H B, Kako T, Liu G G and Ye J H 2016 *Nano Energy* **28** 158–63
[9] Ding N, Xu J Q, Zhang Q, Su J W, Gao Y, Zhou X and Zhai T Y 2018 *Appl. Mater. Interfaces* **10** 10296–303
[10] Kang J S, Wu H and Hu Y 2017 *Nano Lett.* **17** 7507–14
[11] Zheng Q Y, Li S, Li C H, Lv Y C, Liu X Y, Huang P Y, Broido D A, Lv B and Cahill D G 2018 *Adv. Funct. Mater.* **28** 1805116
[12] Varley J B, Miglio A, Ha V, Setten M J, Rignanese G and Hautier G 2017 *Chem. Mater.* **29** 2568–73
[13] Jiang H R, Shyy W, Liu M, Liu L, Wu M C and Zhao T S 2017 *J. Mater. Chem.* A **5** 672–9
[14] Onat B, Hallioglu L, ipek S and Durgun E 2017 *J. Phys. Chem.* C **8** 4583–92
[15] Bhattacharyya G, Choudhuri I and Pathak B 2018 *Phys. Chem. Chem. Phys.* **20** 22877
[16] Padavala B, Frye C D, Wang X, Raghothamachar B and Edgar J H 2016 *J. Cryst. Growth* **449** 15–21
[17] Li G L, Abbott J K, Brasfield J D, Liu P Z, Dale A, Duscher G, Rack P D and Feigerle C S 2015 *Appl. Surf. Sci.* **327** 7–12
[18] Kumashiro Y, Enomoto T, Sato K, Abe Y, Hirata K and Yokoyama T 2004 *J. Solid State Chem.* **177** 529–32

[19] PERET J L 1964 *J. Am. Ceram. Soc.* **47** 44–6
[20] Woo K, Lee K and Kovnir K 2016 *Mater. Res. Express* **3** 7
[21] Mukhanov V A, Vrel D, Sokolov P S, Godec Y L and Solozhenko V L 2016 *Dalton Trans.* **45** 10122–6
[22] Cai S *et al* 2018 *npj Quantum Mater.* **3** 62
[23] Zhu L, Liu H Y, Pickard J, Zou G T and Ma Y M 2014 *Nature Chem.* **6** 644–8
[24] Silva J L, Oliveira A C, Vieira T C, Oliveira G A, Suarez M C and Foguel D 2014 *Chem. Rev.* **114** 7239–67
[25] Williams F V and Ruehrwein R A 1960 *J. Am. Ceram. Soc.* **82** 1330–2
[26] Chu T L, Jackson J M, Hyslop A E and Chu S C 1971 *J. Appl. Phys.* **42** 420–4
[27] Sugimoto H, Fujii M and Imakita K 2014 *RSC Adv.* **5** 8427–31
[28] Huber S P *et al* 2016 *Opt. Mater. Express* **6** 3946–59
[29] Huber S P *et al* 2017 *Phys. Chem. Chem. Phys.* **19** 8174–87
[30] Cui S X, Feng W X, Hu H Q, Feng Z B and Wang Y X 2009 *Comput. Mater. Sci.* **44** 1386–9
[31] Kumar M 2003 *Physica* B **212** 391–4
[32] Solozhenko V L, Kurakevych O O, Godec Y L, Kurnosov A V and Oganov A R 2014 *J. Appl. Phys.* **116** 033501
[33] Wettling W and Windscheif J 1984 *Solid State Commin.* **50** 33–4
[34] Suzuki T, Yagi T and Akimoto S 1983 *J. Appl. Phys.* **54** 748–51
[35] Hauge H I T *et al* 2015 *Nano Lett.* **15** 5855–60
[36] Sanjurjo J A, Lopez-Cruz E, Vogl P and Cardona M 1983 *Phys. Rev.* B **28** 4579–84
[37] Wu K D *et al* 2016 *Nature Commun.* **7** 12952
[38] Pomeroy J W, Kuball M, Hubel H, van Uden N W A and Dunstan D J 2004 *J. Appl. Phys.* **96** 910–2